Published in final edited form as:
Anal Bioanal Chem. 2010 February ; 396(3): 1143–1152. doi:10.1007/s00216-009-3313-8.

Use of the quartz crystal microbalance to monitor ligand-induced conformational rearrangements in HIV-1 envelope protein gp120

Hyun-Su Lee,
Department of Chemistry, Drexel University, 3141 Chestnut Street, Philadelphia, PA 19104, USA

Mark Contarino,
Department of Biochemistry and Molecular Biology, Drexel University College of Medicine, 245 N. 15th Street, Philadelphia, PA 19102, USA

M. Umashankara,
Department of Biochemistry and Molecular Biology, Drexel University College of Medicine, 245 N. 15th Street, Philadelphia, PA 19102, USA

Arne Schön,
Department of Biology, Johns Hopkins University, 3400 N. Charles Street, Baltimore, MD 21218, USA

Ernesto Freire,
Department of Biology, Johns Hopkins University, 3400 N. Charles Street, Baltimore, MD 21218, USA

Amos B. Smith III,
Department of Chemistry, University of Pennsylvania, 231 S. 34th Street, Philadelphia, PA 19104, USA

Irwin M. Chaiken, and
Department of Biochemistry and Molecular Biology, Drexel University College of Medicine, 245 N. 15th Street, Philadelphia, PA 19102, USA

Lynn S. Penn
Department of Chemistry, Drexel University, 3141 Chestnut Street, Philadelphia, PA 19104, USA
lynn.s.penn@drexel.edu

Abstract

We evaluated the potential of a quartz crystal microbalance with dissipation monitoring (QCM-D) to provide a sensitive, label-free method for detecting the conformational rearrangement of glycoprotein gp120 upon binding to different ligands. This glycoprotein is normally found on the envelope of the HIV-1 virus and is involved in viral entry into host cells. It was immobilized on the surface of the sensing element of the QCM-D and was exposed to individual solutions of several different small-molecule inhibitors as well as to a solution of soluble form of the host cell receptor to which gp120 binds. Instrument responses to ligand-triggered changes were in qualitative agreement with conformational changes suggested by other biophysical methods.

Correspondence to: Lynn S. Penn.

Keywords

Quartz crystal microbalance (QCM-D); human immunodeficiency virus 1 (HIV-1); ligand-gp120 complex; s-CD4

Introduction

The present paper puts forth the hypothesis that the quartz crystal microbalance with the capability for monitoring dissipation (QCM-D) can provide reliable and direct detection of ligand-triggered conformational rearrangement of gp120, a protein normally found on the surface of the viral envelope of HIV-1. Prior work by others on the changes exhibited by the protein calmodulin upon treatment with calcium ions demonstrated that the QCM technique was suitable for investigation of conformational change [1,2]. The QCM-D technique is based upon a piezoelectric quartz crystal that is set into vibration by an electrical pulse. As does a plucked string on a stringed instrument, the bare crystal vibrates strongly at first, and then the vibrational amplitude decreases until vibration stops. Then another electrical pulse is delivered to set it into vibration again. The decrement in amplitude with each cycle of vibration is a measure of the dissipation, or loss, of the energy imparted to the crystal by the initial electrical pulse. In QCM-D, the crystal is pulsed into vibration several times per second, making data acquisition is essentially continuous. The value of the vibrational frequency (Hz), as well as that of the dissipation (a dimensionless ratio of successive amplitudes), is governed by the dimensions of the crystal and the material from which it is made. The bare quartz crystal, being a small object made of stiff, highly elastic material, has a high resonant frequency and low dissipation. This changes when substances are coupled to the crystal, by virtue of either chemical bonding or intimate contact [3–8]. When the substance is an ultrathin (a few nanometers) layer with very high elastic character, the frequency will be lowered noticeably but the dissipation will remain the same as that of the bare crystal [3]. By contrast, if the layer coupled to the quartz crystal has a high viscous character, both frequency and dissipation will change noticeably [9–17]. If the layer coupled to the quartz crystal is not purely elastic but has viscous character, it is termed viscoelastic and exhibits dissipation that is much higher than that of the bare crystal and that indicates the amount of viscous character in the layer.

The ability of the QCM-D to demonstrate conformational change is nicely illustrated by the well-known collapse of a polymer brush upon change from good solvent to nonsolvent [18]. A polymer brush is a layer of polymer chains, each attached by one end to a solid surface -- in this case to the surface of the quartz crystal. In the traditional brush, where the polymer chains are infused by good solvent, the chains stretch away from the surface to which they are attached. When the solvent is switched to a very poor solvent or a nonsolvent, the chains collapse, flat, onto the surface. That is, this change of solvent converts a thick, viscous and solvent-infused layer into an ultrathin, elastic layer from which the solvent has been expelled. Figure 1 shows the QCM-D response for this change of conformation; the frequencies, $\Delta f_n/n$, normalized for mode number, n, increase and become superimposed, and the ΔD-values all decrease to below 2×10^{-6} (a negligible difference from the dissipation of the bare crystal). These changes are the mark of a transition from a thick viscous layer to an ultrathin elastic layer, *without any change in the number of polymer chains attached to the surface of the crystal*. As can be seen in Figure 1, the collapse of the brush is reversible upon replacement of the nonsolvent with good solvent, whereupon the frequencies all decrease to their original values and the ΔD-values increase to their original level.

We wished to apply QCM-D to assess the changes in the viscoelastic properties of immobilized gp120, a glycoprotein found on the surface of the viral envelope of HIV-1, upon exposure to different ligands. The infection of host cells by HIV-1 is believed to depend on coordinated

conformational rearrangements in gp120, a glycoprotein found on the surface of the viral envelope of HIV-1, when it binds to receptors located on cell surfaces. The sequence of molecular events at the virus-cell synapse begins with the binding of gp120 to CD4, a receptor domain on the surface of the T-cell or macrophage. Binding to CD4 triggers a conformational change in gp120 that enhances its binding to a co-receptor CCR5 (or, in some cases, CXCR4) on the surface of the T-cell or macrophage. Binding of gp120 to the co-receptor leads to further conformational changes that uncover gp41, a glycoprotein partially buried in the viral envelope. These changes lead to structural rearrangements in the viral envelope that help bring it and host cell membrane close enough to fuse together [19–26]. Prevention or modification of the cascade of conformational changes, starting with that of gp120, is believed to be one strategy for treatment of HIV-1 infection in humans. The search for ligands, called inhibitors, that divert fusion-enabling conformational rearrangements of the glycoproteins on surface of the viral envelope, either competitively or allosterically, is an active area of current research. We wanted to evaluate the potential of QCM-D to contribute to a better understanding of the conformational changes in this glycoprotein and to assist in identifying synthetic ligands that could prevent this conformational change.

The binding of the CD4 ligand to gp120 has been studied by both X-ray crystallography [27, 28] and cryo-electron tomography [29,30]. These two static techniques have provided important structural information about gp120 and also about the site in gp120 to which CD4 binds. However, they have not been able to provide a qualitative determination of the overall conformational change that occurs when the ligand binds. In addition, neither technique is able to track the process of binding in real time. By contrast, QCM-D is able to continuously monitor the changes in viscoelastic properties of a given layer of immobilized gp120 molecules as various ligands bind to it. The only other technique that can monitor the overall binding process within a given sample of gp120 molecules is isothermal titration calorimetry (ITC), a technique that measures thermodynamic parameters of the binding process [31–35]. Because conformational change in a system is always accompanied by changes in the thermodynamic properties of the system, ITC provides an excellent basis for comparison with QCM-D data. The ligands selected for use in the present QCM-D study were those for which ITC data were available. The results of the study described in the present paper showed that the changes in viscoelasticity observed with QCM-D were consistent with changes in entropy measured with ITC. These results confirm the appropriateness of QCM-D for the study of ligand-induced conformational rearrangement in gp120.

Experimental

Instrumentation

The quartz crystal microbalance used in this work was model E4 QCM-D from Q-Sense Inc., (Gothenburg, Sweden). The sensing element is a replaceable AT-cut piezoelectric quartz disc (14 mm in diameter and 0.3 mm thick) that vibrates in-plane at a characteristic resonant frequency and overtones. The disc is mounted in a flow cell, and, to use a coin analogy, the “heads” side of the disc is in contact with a solution of the substance of interest while the “tails” side, isolated from the flowing solution by a gasket, is patterned with a deposited metal electrode. The frequency and damping of the disc change when mass is coupled to or is decoupled from the sensing surface (the “heads” side) and the electrode on the “tails” side sends this frequency and damping information continuously to the data collection system. To facilitate chemical derivatization of the surface of the disc, we used quartz discs having “heads” sides coated with a 100-nm thick layer of vapor-deposited gold. Replacement piezoelectric quartz discs were obtained from Q-Sense, Inc.; they had natural resonant frequencies of 4.95 MHz, with 1% crystal-to-crystal variation. The sensitivity of the instrument is 1.77 ng/cm^2 of mass deposited, equivalent to a response of 0.1 Hz. The instrument reports $\Delta f_n/n$, change in frequency normalized by mode number, n, and ΔD, change in dissipation, as a function of time

for each vibrational mode monitored. Except where noted, all procedures were done at 21°C. The flow-through mode was used because it allowed real-time, uninterrupted monitoring of immobilization of the protein, binding of the ligand, and buffer washing. Two flow systems, driven by a peristaltic pump, were used: the standard recirculating system suitable for liquid volumes of tens of mL and flow rates of tens of μ*L*/min, and a custom-constructed, nonrecirculating system miniaturized for use with small volumes and near-zero flow rates, as required when the materials of interest are available in very limited quantities or are vulnerable to damage at high flow rates.

Materials

All organic solvents, concentrated acids, and H_2O_2 were purchased from Fisher, Pittsburgh, PA. Anhydrous ethanol (>99.9%) was purchased from Pharmco-Aaper, Shelbyville, KY. The 3,3'dithiobis[N-(5-amino-5-(carboxypentyl) propionamide-N,N'-diacetic acid]dihyrochloride, abbreviated hereafter as NTA, was purchased from Dojindo Molecular Technologies, Rockville, MD. Nickel(II) sulfate (99.99%) was purchased from the Aldrich Chemical Co. The vector for expression of glycoprotein HIV-1_{YU-2}gp120 containing a C-terminal hexahistidine tag was obtained from the laboratory of Dr. Joseph Sodroski, Dana Farber Cancer Institute, Boston, MA. HIV-1_{YU-2}gp120 was produced by transfection of the aforementioned vector into 293Freestyle cells with 293fectin according to manufacturer's protocols and was purified by means of immobilized metal affinity chromatography and gel filtration chromatography. Size, purity and functionality were verified by sodium dodecyl sulfate polyacrylamide gel electrophoresis and surface plasmon resonance biosensing. The sCD4, the soluble extracellular portion of the protein in the T-cell or macrophage to which gp120 binds, was obtained by means of recombinant cell expression [36]. Small molecules used for binding to gp120 are shown in Figure 2. These were NBD-556 and BMS-806, synthesized by previously reported methods [33,37]. The peptide HNG-156 was produced by solid phase peptide synthesis followed by on-resin introduction of a ferrocene-substituted triazole to the proline residue [38]. For use as a negative control, a nonbinding peptide analog of HNG-156 was prepared [39].

Cleaning of surface and stabilization of crystal in flow cell

The top (gold-coated) surface of the quartz crystal was cleaned with piranha solution (70 vol % concentrated H_2SO_4 and 30 vol% H_2O_2) for 30 min. The surface was rinsed alternately with water and acetone, and was dried in flowing argon. The cleaned, gold-coated crystal was mounted in the flow cell of the QCM-D instrument. The crystal was subjected to further rinsing with flowing anhydrous ethanol that had been freshly distilled under argon. Rinsing at a flow rate of 34 μ*L*/min and at 40°C was continued for 1 h, after which the temperature of the flow cell was adjusted to 21°C and anhydrous ethanol was allowed to flow until a stable baseline was established (typically 1–2 h). The values of $\Delta f_n/n$ and ΔD in the QCM-D instrument were set to zero in preparation for monitoring of subsequent procedures.

Derivatization of surface

Protein containing a hexahistidine tag can be immobilized on a surface derivatized with NTA to which nickel has been chelated [40,41]. Therefore, derivatization of the stabilized, gold-coated crystal was carried out in the flow cell of the QCM-D. Upon exposure of the gold surface to a flowing solution of 1.0 mg of NTA in 50 mL of anhydrous ethanol, a self-assembled monolayer of NTA formed immediately (as indicated by a rapid decrease in vibrational frequency of the crystal), attached to the gold surface by disulfide groups and topped by the carboxylic acid groups of the NTA. After 15 h, the self-assembled monolayer had reached maximum density, and anhydrous ethanol was allowed to flow through the cell for 2 h to remove any non-attached NTA from the surface of the crystal and to clear it from the tubing and flow cell. This highly reproducible monolayer was shown by the QCM-D instrument to be highly

elastic in character (no difference in dissipation from the bare crystal). Therefore, the Sauerbrey equation, which converts the frequency shift corresponding to an elastic deposited layer to mass, in ng/nm^2, could be used [18,42]. The resultant mass, combined with the molecular weight of the molecular species composing the monolayer, yielded a density of 3.84 NTA moieties per nm^2, indicating a well-packed monolayer with molecular backbones approximately perpendicular to the gold surface.

Chelation of nickel by NTA

The rinsed, NTA-derivatized crystal was removed from the flow cell, dried with argon and repositioned in the non-recirculating flow-cell system. The mounted crystal was exposed to pure water at a flow rate of 1 μ*L*/min until a stable baseline was established. The $\Delta f_n/n$- and ΔD-values were set to zero, and the NTA-derivatized crystal was exposed to a solution of 0.41 *mM* NaOH in de-ionized water at a flow rate of 1 μ*L*/min to neutralize the carboxylic acid groups. Flow was continued until no further mass change occurred, indicating that all of the protons on the carboxylic acid had been replaced by Na^+ ions. After this, the flowing solution was switched to 0.26 *mM* $NiSO_4$ in de-ionized water to allow chelation of Ni^{2+} ions by the carboxylate groups. Again, chelation was indicated by an initial frequency change that leveled off, once the carboxylate groups of the NTA were saturated with Ni^{2+}. A flowing solution of 0.44 *mM* NaCl in de-ionized water was passed over the surface to flush excess $NiSO_4$ from the flow cell and tubing.

Immobilization of gp120

The solution passing through the flow cell was switched from aqueous NaCl to phosphate-buffered saline (PBS). The flow rate was adjusted downward to 0.4 μ*L*/min, a flow rate that was maintained for all subsequent steps of the experimental protocol. This was done because an extremely low rate of flow - nearly zero - was required in order to avoid disruption of the protein by mechanical shearing action of flowing liquid. After the system was stabilized in flowing PBS, the baseline was reset to zero, in preparation for monitoring of the immobilization of gp120. (It is the hexahistidine tag on the C-terminus of gp120 that coordinates with the nickel ions in the Ni-NTA complex attached to the surface of the crystal.) Then 168 μ*L* of gp120 solution (0.5 μ*M* in PBS) was introduced into the flow line. It took approximately 8 h for this volume of solution to pass into, through, and out of the flow cell, so that gp120 in solution was in contact with the surface of the crystal for several hours. The gp120 solution was followed by pure PBS, to rinse the system. Rinsing was continued for ~ 10 h to rinse residual gp120 from the flow cell and tubing. Figure 3 shows in cartoon form the sequence of steps leading to immobilization of gp120 and subsequent binding of ligand. The immobilized gp120 takes the form of a randomly distributed monolayer on the derivatized surface of the crystal. The typical scatter among replicate layers of immobilized gp120 on individual quartz crystals, each of area ~1.54 cm^2, was ~40%.

Exposure of ligand solutions to immobilized gp120

The mass of the ligand used in the experiments needed to be optimized so that the instrument response would be due mainly to binding of the ligand to immobilized gp120 and would not be dominated by physical adsorption of the ligand to the underlying surface. This optimization was done by trial and error, and the result was a modest excess of ligand over that needed for one-to-one binding of ligand to gp120, delivered in a small total volume at low concentration. The molecular weights and concentrations of the solutions of ligands used in this study are listed in Table 1. The gp120 is much more massive, with a molecular weight of 120,000 g/mol. Because the QCM-D responds to changes in mass coupled to the surface of the sensing element, total mass of ligand used had to be consistent from experiment to experiment to achieve comparable signal size; as a result, the molarities in the table are inverse to the molecular

weights. In each experiment, 40 μ*L* of the ligand solution was introduced into the flow system at a rate of 0.4 μ*L*/min, the lowest rate that could be achieved with the experimental apparatus used. At this flow rate, it took two hours for the ligand solution to pass from the reservoir through the tubing to enter the flow cell and reach the surface of the crystal. The ligand solution was followed by pure PBS to rinse the cell and evaluate dissociation of the ligand from the immobilized gp120. Experiments with a given ligand were typically done twice. Kinetics information could not be obtained from these experiments, because the flow rate was so low that mass transport from the bulk solution to the immobilized was the limiting step. In fact, because of the transport-dependence and the low flow rate, rebinding and re-dissociation could occur repeatedly during rinsing, making it impossible to make any quantitative judgments about dissociation of the complex in these experiments. Control studies, in which ligands were exposed to the Ni-NTA-derivatized surface of the crystal that contained no immobilized gp120, were also done.

Results and discussion

As mentioned in the introduction, we used ligands for gp120 for which thermodynamic data were available in the literature. Figure 4 shows thermodynamic data obtained by means of isothermal titration calorimetry (ITC) for the binding of four ligands to gp120. The negative values of ΔG per mole for all four ligands in Figure 4 indicate that binding is a spontaneous process at the experimental temperature (25°C). Positive values of $-T\Delta S$ correspond to negative values of ΔS. The decrease in molar entropy for the binding of sCD4 to gp120 is one of the largest detected for protein-protein binding and has been interpreted as a large increase in structural order of the gp120 [32,35]. The ligands NBD-556 and HNG-156 also produce a decrease in molar entropy upon binding to gp120, whereas the ligand BMS-806 produces an increase in entropy. Binding of sCD4, NBD-556 and, to some extent, HNG-156 to gp120 is also associated with very large and negative heat capacity changes that together with the unusually large and favorable enthalpy and unfavorable entropy changes suggest association processes where the ligands induce large conformational structuring upon binding [43]. As reported previously, sCD4 and NBD-556 structure about 130 and 67 residues, respectively, in gp120 [33,44]. To sum up, sCD4, NBD-556, and HNG-156, but not BMS-806, trigger an ordering of the gp120. The small favorable ΔS associated with the binding of BMS-806 is consistent with the binding and hydrophobic burial of a small molecule to a protein coupled to no or very small conformational changes.

The QCM-D technique is designed to reveal changes in the viscoelastic properties of an immobilized layer. Because conformational change in a monolayer of protein molecules would be expected to cause a change in the viscoelastic properties of the layer, the QCM-D technique should provide information about these changes. Thus, when immobilized gp120 is exposed to solutions of sCD4, NBD-556, HNG-156, and BMS-806, respectively, we should expect the QCM-D to reveal changes in the viscoelasticity of the immobilized layer that are consistent with the changes in entropy found by means of ITC for each of the ligands.

We first present results of control studies done to evaluate the extent of physical adsorption of ligands to the bare Ni-NTA-derivatized surface, in the absence of immobilized gp120. Conditions used for the control studies were the same as those used for the experimental studies, i.e., those with immobilized gp120. Figure 5a shows the response of the QCM-D instrument when a solution of NBD-556 in PBS was introduced (at arrow labeled **E**) into the flow cell, subsequent to pure, flowing PBS. Figure 5b shows the data for introduction of a solution BMS-806 in PBS. Physical adsorption of the ligand molecules to the Ni-NTA-derivatized surface produced a decrease in $\Delta f_n/n$ on the order of 1 Hz and simultaneous increase in ΔD on the order of 0.5×10^{-6}. The changes due to physical adsorption were much smaller than the changes due to ligand binding (shown later), so that any physical adsorption of ligand to

partially accessible surface under the immobilized gp120 would not interfere with interpretation of the results. Rinsing with pure PBS was begun at **R** just after $\Delta f_n/n$ had reached a minimum and ΔD had reached a maximum. (The approach of a minimum or maximum in the data-dense traces can be anticipated easily by expansion of the data-dense horizontal scale during the experiment.) Rinsing resulted in a return of $\Delta f_n/n$ and ΔD nearly to their original values, signaling desorption of nearly all the adsorbed molecules. The gradual nature of the adsorption-desorption process was a consequence of the natural omni-directional diffusion of the molecule in dilute solution, overlaid on the very low but directional flow rate. The other ligands used in our study, the peptide HNG-156 and the protein sCD4, showed a similar small amount of physical adsorption to the Ni-NTA-derivatized surface, but these molecules could not be removed completely with flowing PBS. This is not unexpected, because peptides and proteins have many sites with which to adsorb Ni-NTA-derivatized surface.

In addition to the above controls, a negative control involving exposure of a nonbinding peptide analog [39] of HNG-156 to immobilized gp120 was conducted. This nonbinding peptide elicited a smooth and gradual decrease in $\Delta f_n/n$ and increase in ΔD, similar to that observed for the physical adsorption of ligands to the Ni-NTA-derivatized surface. The response of the QCM-D to introduction of this negative control was characteristic simply of added mass, probably physical adsorption of the peptide to the exposed portions of the surface between the immobilized gp120 molecules. Rinsing with PBS readily removed all the peptide molecules from the system.

Figure 6 shows the QCM-D data from experiments in which the four binding ligands depicted in Figure 4 were exposed to monolayers of immobilized gp120. So that all the features of QCM-D data can be explained, Figure 6 shows the complete history of each experiment, from immobilization of gp120 on the surface of the derivatized quartz crystal all the way to the final rinse to clear the flow cell of any free species. The baseline was established at zero for both $\Delta f_n/n$ (n = 3, 5, 7) and ΔD, and then the gp120 solution was connected to the flow cell. There is a distinct drop in $\Delta f_n/n$ as the gp120 is immobilized on the Ni-NTA-derivatized surface of the crystal. By approximately 12 hours, the layer of immobilized gp120 has been fully constructed and can be seen to be *visco*elastic rather than elastic. This is indicated by the separation between the frequency traces for n = 3, 5, and 7 and ΔD-values greater than 2×10^{-6}. Viscoelastic character, as opposed to elastic character, is exactly what is expected for a bulky, solvent-infused protein. The immobilized gp120 was rinsed for approximately ten hours with pure, flowing phosphate-buffered saline before the ligand solution was introduced at **E**. The relative constancy of $\Delta f_n/n$ (n = 3, 5, 7) and ΔD during this rinsing operation verified that gp120 was not removed from the surface by the shear stress associated with laminar flow. (Not shown are results in which rinsing at flow rates ten times higher, which very slowly detached the gp120 from the Ni-NTA-derivatized surface.) Underlying all of the features of the QCM-D data are small and gradual decreases in frequency and increases in dissipation, sometimes barely perceptible, that reflect a slight amount of instrument drift over long operating times.

In Figures 6a, 6b, and 6c, the QCM-D shows a large response to the introduction of ligands sCD4, NBD-556 and HNG-156, respectively, at **E**. The traces for $\Delta f_n/n$ increase and those for ΔD decrease. These changes are in the *opposite* directions from those expected simply from the addition of mass (of the ligand) to the gp120 layer. For Figures 6a, 6b, and 6c, the observed decrease in ΔD at **E** indicates that the immobilized layer now has less viscous character than before and has become more elastic. The convergence of the $\Delta f_n/n$-traces for the three vibrational modes, n = 3, 5, and 7, also indicates an increase in elastic character (complete superposition corresponds to a highly elastic layer) and a decrease in viscous character. The increases in $\Delta f_n/n$-values are also consistent with a loss of mass coupled to the surface of the sensor, most likely that of solvent within the immobilized layer.

Figure 6d shows the QCM-D data for BMS-806, the fourth ligand in our test series. The instrument response to the introduction this ligand at **E** is entirely different from the response to the first three ligands. There is a *decrease* in $\Delta f_n/n$ and an *increase* in ΔD, of the gp120 upon introduction of BMS-806. A portion of the observed decrease in $\Delta f_n/n$ and increase in ΔD can be attributed simply to the added mass of BMS-806 as it couples to the immobilized layer of gp120. However, comparison with Figure 5 shows that, even at most, the added mass cannot account completely for the observed decrease in $\Delta f_n/n$ and increase in ΔD.

Rinsing with pure PBS was begun at **R** for all four test ligands, just after $\Delta f_n/n$ reached a maximum in Figures 6a, 6b, and 6c, and reached a minimum in Figure 6d. The complexes made by each of the four ligands with the immobilized gp120 responded differently to rinsing; some complexes dissociated readily and other complexes appeared to resist dissociation. However, the immobilzed gp120 remained intact. As mentioned previously, because mass transport was rate limiting and because re-binding could occur constantly during rinsing, no conclusions regarding dissociation constants can be drawn from the data reported here.

Although QCM-D *directly* probes the changes in mechanical properties of the layer coupled to the surface of the sensing element, we still must rely on the fundamental principles of mechanics to interpret the data. Three of the ligands, sCD4, NBD-556, and HNG-156, used in this study caused the frequency of the vibrating crystal to increase and the dissipation to decrease. This meant that the binding of the ligands to the gp120 brought about a decrease in the viscous character and an increase in the elastic character of the immobilized layer. This could have happened in either or both of two ways. Either the component of the layer having the most viscous character, i.e., the aqueous solvent, was partially expelled, or the immobilized macromolecules themselves assumed conformations that were better able to respond elastically to the small deformation caused by each oscillation of the vibrating quartz crystal. In fact, these two ways are not at all mutually exclusive. Molecular conformations that are better able to respond elastically to deformation require stronger interactions, i.e., closer distances, between different segments of the macromolecule. In turn, reduction of segment-to-segment distances requires expulsion of some of the intervening solvent. The simultaneous reduction of distances and expulsion of solvent constitutes a contraction of part or all of the macromolecule. Clearly, according to the QCM-D, three of the ligands used in the present study caused some degree of contraction, which also could be termed "ordering" or "structuring," in the gp120. For one of the ligands in this study, the QCM-D indicated changes in the opposite direction. This ligand, BMS-806, triggered a slight decrease in the elastic character and an increase in the viscous character of the layer, suggesting an expansion, or "destructuring," of the immobilized gp120 monomers. The changes in viscoelasticity of the gp120 layer, triggered by the ligands, is information that is not provided by any other technique.

Like QCM-D, ITC gives indirect evidence of conformational change through *direct* measurement of thermal changes in a solvent-solute system. These changes, too, must be interpreted. The change in entropy, ΔS, associated with a binding event has different components, the most important being the entropy of solvation and the conformational entropy. The release of solvent water upon binding contributes favorably to the solvation entropy whereas the reduction in number of conformations of the ligand and macromolecule corresponds to a decrease in the conformational entropy. Binding of sCD4 induces a massive structuring of gp120 associated with unusually large changes in favorable enthalpy and unfavorable entropy. The event resembles protein folding, where the unfavorable conformational entropy change is larger than the favorable solvation entropy and overall process is driven by the large change in favorable enthalpy associated with the formation of bonds between previously distant residues. ITC measurements have shown that a similar structuring of gp120 is observed upon binding of certain ligands such as HNG-156 and, in particular, the CD4 mimic, NBD-556, whereas BMS-806 binds without inducing any

significant conformational changes. Clearly, the findings acquired by the QCM-D technique are in good qualitative agreement with the findings of the ITC technique.

Conclusion

The QCM-D technique was shown in the experiments reported here to be able to reveal changes in the viscoelastic properties of surface immobilized gp120, a glycoprotein normally found on the envelope of the HIV-1 virion. The ligand-triggered changes in viscoelastic character were indicative of conformational change in surface-immobilized gp120. The QCM-D technique revealed conformational ordering in qualitative agreement with that indicated by the ΔS-values of isothermal titration calorimetry for the binding of the same ligands to gp120. The consistency found between the two methods verifies that QCM-D is a valid and useful technique for the study of conformational change triggered by binding of certain ligands to large, immobilized protein. Furthermore, by probing the viscoelastic properties of the immobilized layer, QCM-D can provide different but complementary information to that provided by ITC. QCM-D is especially attractive because it is label-free, directly probes the layer coupled to the quartz crystal of the instrument, and does not probe the bulk medium beyond the coupled layer. That both of these techniques, which measure different properties, lead to the same interpretation, strengthens the suggestion made by others that indeed there is a structural ordering, or a contraction, of the gp120 when certain ligands bind to it. In sum, the QCM-D data supports the ITC data and provides added meaning.

Acknowledgments

The authors thank Dr. Jason Cox, Department of Chemistry, University of Pennsylvania, for supplying BMS-806. They also thank National Institutes of Health 5P01GM56550-12, National Institutes of Health R21AI071965-01, and International Partnership for Microbicides/USAID for funding.

References

1. Wang X, Ellis JS, Lyle EM, Sundaram P, Thompson M. Conformational chemistry of surface-attached calmodulin detected by acoustic shear wave propagation. Mol BioSyst 2006;2:184–192. [PubMed: 16880936]
2. Furusawa H, Komatsu M, Okahata Y. In situ monitoring of conformational changes of and bindings to calmodulin on a 27 MHz quartz crystal microbalance. Anal Chem 2009;81:1841–1847. [PubMed: 19182898]
3. Sauerbrey G. The use of quartz crystal oscillators for weighing thin layers and for micro-weighing. Z Phys 1959;155:206–222.
4. Ward MD, Buttry DA. In situ interfacial mass detection with piezoelectric transducers. Science 1990;249:1000–1007. [PubMed: 17789608]
5. Schneider TW, Buttry DA. Electrochemical quartz crystal microbalance studies of adsorption and desorption of self-assembled monolayers of alkyl thiols on gold. J Am Chem Soc 1993;115:12391–12397.
6. Keller CA, Glasmastar K, Zhdanov VP, Kasemo B. Formation of supported membranes from vesicles. Phys Rev Lett 2000;84:5443–5446. [PubMed: 10990964]
7. Vogt BD, Lin EK, Wu W, White CC. Effect of film thickness on the validity of the sauerbrey equation for hydrated polyelectrolyte films. J Phys Chem B 2004:12685–12690.
8. Vogt BD, Soles CL, Lee H, Lin EK, Wu W. Moisture absorption and absorption kinetics in polyelectrolyte films: influence of film thickness. Langmuir 2004;20:1453–1458. [PubMed: 15803734]
9. Rodahl M, Hook F, Krozer A, Brzezinski P, Kasemo B. Quartz-crystal microbalance setup for frequency and Q-factor measurements in gaseous and liquid environments. Rev Sci Instrum 1995;66:3924–3930.

10. Caruso F, Furlong DN, Kingshott P. Characterization of ferritin adsorption onto gold. J Colloid Interface Sci 1997;186:129–140. [PubMed: 9056316]
11. Hook F, Rodahl M, Brzezinski P, Kasemo B. Energy dissipation kinetics for protein and antibody-antigen adsorption under shear oscillation on a quartz crystal microbalance. Langmuir 1998;14:729–734.
12. Hook F, Kasemo B, Nylander T, Fant C, Sott K, Elwing H. Variations in coupled water, viscoelastic properties, and film thickness of a Mefp-1 protein film during adsorption and cross-linking: a quartz crystal microbalance with dissipation monitoring, ellipsometry, and surface plasmon resonance study. Anal Chem 2001;73:5796–5804. [PubMed: 11791547]
13. Voinova MV, Rodahl M, Jonson M, Kasemo B. Viscoelastic acoustic response of layered polymer films at fluid-solid interfaces: continuum mechanics approach. Physica Scripta 1999;59:391–396.
14. Hook F, Voros J, Rodahl M, Kurrat R, Boni P, Ramsden JJ, Textor M, Spencer ND, Tengvall P, Gold J, Kasemo B. A comparative study of protein adsorption on titanium oxide surfaces using in situ ellipsometry, optical waveguide lightmode spectroscopy, and quartz crystal microbalance/dissipation. Colloids and Surfaces B - Biointerfaces 2002;24:155–170.
15. Moya SE, Brown AA, Azzaroni O, Huck WTS. Following polymer brush growth using the quartz crystal microbalance technique. Macromol Rapid Commun 2005;26:1117–1121.
16. Ma H, Textor M, Clark RL, Chilkoti A. Monitoring kinetics of surface initiated atom transfer radical polymerization by quartz crystal microbalance with dissipation. Biointerphases 2006;1:35–39. [PubMed: 20408613]
17. He J, Wu Y, Wu J, Mao X, Fu L, Qian T, Fang J, Xiong C, Xie J, Ma H. Study and application of a linear frequency–thickness relation for surface-initiated atom transfer radical polymerization in a quartz crystal microbalance. Macromolecules 2007;40:3090–3096.
18. Lee H, Penn LS. *In situ* study of polymer brushes as selective barriers to diffusion. Macromolecules 2008;41:8124–8129.
19. Barre-Sinoussi F, Chermann JC, Rey F, Nugeyre MT, Chamaret S, Gruest J, Dauguet C, Axler-Blin C, Vezinet-Brun F, Rouzioux C, Rozenbaum W, Montagnier L. Isolation of a T-lymphotropic retrovirus from a patient at risk for acquired immune deficiency syndrome (AIDS). Science 1983;220:868–871. [PubMed: 6189183]
20. Chan DC, Kim PS. HIV entry and its inhibition. Cell 1998;93:681–684. [PubMed: 9630213]
21. Dalgleish AG, Beverley PCL, Clapham PR, Crawford DH, Greaves MF, Weiss RA. The CD4 (T4) antigen is an essential component of the receptor for the AIDS retrovirus. Nature 1984;312:763–767. [PubMed: 6096719]
22. Deng H, Liu R, Ellmeier W, Choe S, Unutmaz D, Burkhart M, Di Marzio P, Marmon S, Sutton RE, Hill CM, Davis CB, Peiper SC, Schall TJ, Littman DR, Landau NR. Identification of a major co-receptor for primary isolates of HIV-1. Nature 1996;381:661–666. [PubMed: 8649511]
23. Doms RW, Moore JP. HIV-1 membrane fusion: targets of opportunity. J Cell Biol 2000;151:F9–F14. [PubMed: 11038194]
24. Jones PL, Korte T, Blumenthal R. Conformational changes in cell surface HIV-1 envelope glycoproteins are triggered by cooperation between cell surface CD4 and co-receptors. J Biol Chem 1998;273:404–409. [PubMed: 9417096]
25. Moore JP, Doms RW. The entry of entry inhibitors: a fusion of science and medicine. Proc Natl Acad Sci USA 2003;100:10598–10602. [PubMed: 12960367]
26. Sullivan N, Sun Y, Sattentau Q, Thali M, Wu D, Denisova G, Gershoni J, Robinson J, Moore J, Sodroski J. CD4-Induced conformational changes in the human immunodeficiency virus type 1 gp120 glycoprotein: consequences for virus entry and neutralization. J Virol 1998;72:4694–4703. [PubMed: 9573233]
27. Kwong PD, Wyatt R, Majeed S, Robinson J, Sweet RW, Sodroski J, Hendrickson WA. Structures of HIV gp120 envelope glycoproteins from laboratory-adapted and primary isolates. Structure 2000;8:1329–1339. [PubMed: 11188697]
28. Kwong PD, Wyatt R, Robinson J, Sweet RW, Sodroski J, Hendrickson WA. Structure of an HIV gp120 envelope glycoprotein in complex with the CD4 receptor and a neutralizing human antibody. Nature 1998;393:648–659. [PubMed: 9641677]

29. Zanetti G, Briggs JAG, Grunewald K, Sattentau QJ, Fuller SD. Cryo-electron tomographic structure of an immunodeficiency virus envelope complex in situ. PLoS Pathogens 2006;2:790–797.
30. Liu J, Bartesaghi A, Borgnia MJ, Sapiro G, Subramaniam S. Molecular architecture of native HIV-1 gp120 trimers. Nature 2008;455:109–113. [PubMed: 18668044]
31. Madani N, Schon A, Princiotto AM, Lalonde JM, Courter JR, Soeta T, Ng D, Wang L, Brower ET, Xiang S, Kwon Y, Huang C, Wyatt R, Kwong PD, Freire E, Smith AB III, Sodroski J. Small-molecule CD4 mimics interact with a highly conserved pocket on HIV-1 gp120. Structure 2008;16:1689–1701. [PubMed: 19000821]
32. Myszka DG, Sweet RW, Hensley P, Brigham-Burke M, Kwong PD, Hendrickson WA, Wyatt R, Sodroski J, Doyle ML. Energetics of the HIV gp120-CD4 binding reaction. Proc Natl Acad Sci USA 2000;97:9026–9031. [PubMed: 10922058]
33. Schon A, Madani N, Klein JC, Hubicki A, Ng D, Yang X, Smith AB III, Sodroski J, Freire E. Thermodynamics of binding of a low-molecular-weight CD4 mimetic to HIV-1 gp120. Biochemistry 2006;45:10973–10980. [PubMed: 16953583]
34. Si Z, Madani N, Cox JM, Chruma JJ, Klein JC, Schon A, Phan N, Wang L, Biorn AC, Cocklin S, Chaiken I, Freire E, Smith AB III, Sodroski JG. Small-molecule inhibitors of HIV-1 entry block receptor-induced conformational changes in the viral envelope glycoproteins. Proc Natl Acad Sci USA 2004;101:5036–5041. [PubMed: 15051887]
35. Leavitt S, Freire E. Direct measurement of protein binding energetics by isothermal titration calorimetry. Curr Opin Struct Biol 2001;11:560–566. [PubMed: 11785756]
36. Tendian SW, Myska DG, Sweet RW, Chaiken IM, Brouillette CG. Interdomain communication of T-cell CD4 studies by absorbance and fluorescence difference spectroscopy measurements of urea-induced unfolding. Biochem 1995;34:6464–6474. [PubMed: 7756278]
37. Wang T, Zhang Z, Wallace OB, Deshpande M, Fang H, Yang Z, Zadjura LM, Tweedie DL, Huang S, Zhao F, Ranadive S, Robinson BS, Gong YF, Ricarrdi K, Spicer TP, Deminie C, Rose R, Wang HH, Blair WS, Shi P, Lin P, Colonno RJ, Meanwell NA. Discovery of 4-benzoyl-1-[(4-methoxy-1H-pyrrolo[2,3-b]pyridin-3-yl)oxoacetyl]-2-(R)-methylpiperazine (BMS-378806): a novel HIV-1 attachment inhibitor that interferes with CD4-gp120 interactions. J Med Chem 2003;46:4236–4239. [PubMed: 13678401]
38. Gopi H, Cocklin S, Pirrone V, McFadden K, Tuzer F, Zentner I, Ajith S, Baxter S, Jawanda N, Krebs FC, Chaiken IM. Introducing metallocene into a triazole peptide conjugate reduces its off-rate and enhances its affinity and anti-viral potency for HIV-1 gp120. J Mol Recognit 2009;22:169–174. [PubMed: 18498083]
39. Umashankara M, Zentner I, McFadden K, Chaiken I. Dept. Biochemistry and Molecular Biology, Drexel University College of Medicine, protocol for preparation of UM-24DW, (Cit-N-N-I-Azp (ferrocene)-W(D)-S), molecular weight = 1136 g/mol. 2009 manuscript in preparation.
40. Chaga GS. Twenty-five years of immobilized metal ion affinity chromatography: past, present and future. J Biochem Biophys Methods 2001;49:313–334. [PubMed: 11694287]
41. Gaberc-Porekar V, Menart V. Potential for using histidine tags in purification of proteins at large scale. Chem Eng Technol 2005;28:1306–1314.
42. Sauerbrey G. The use of quartz crystal oscillators for weighing thin layers and for microweighing. Z. Phys 1959;155:206–222.
43. Luque I, Freire E. Structure-based prediction of binding affinities and molecular design of peptide ligands. Methods Enzymol 1998;295:100–122. [PubMed: 9750216]
44. Leavitt SA, Schön A, Klein JC, Manjappara U, Chainken IM, Freire E. Interactions of HIV-1 proteins gp120 and Nef with cellular partners define a novel allosteric paradigm. Curr Protein Pept Sci 2004;5:1–8. [PubMed: 14965316]

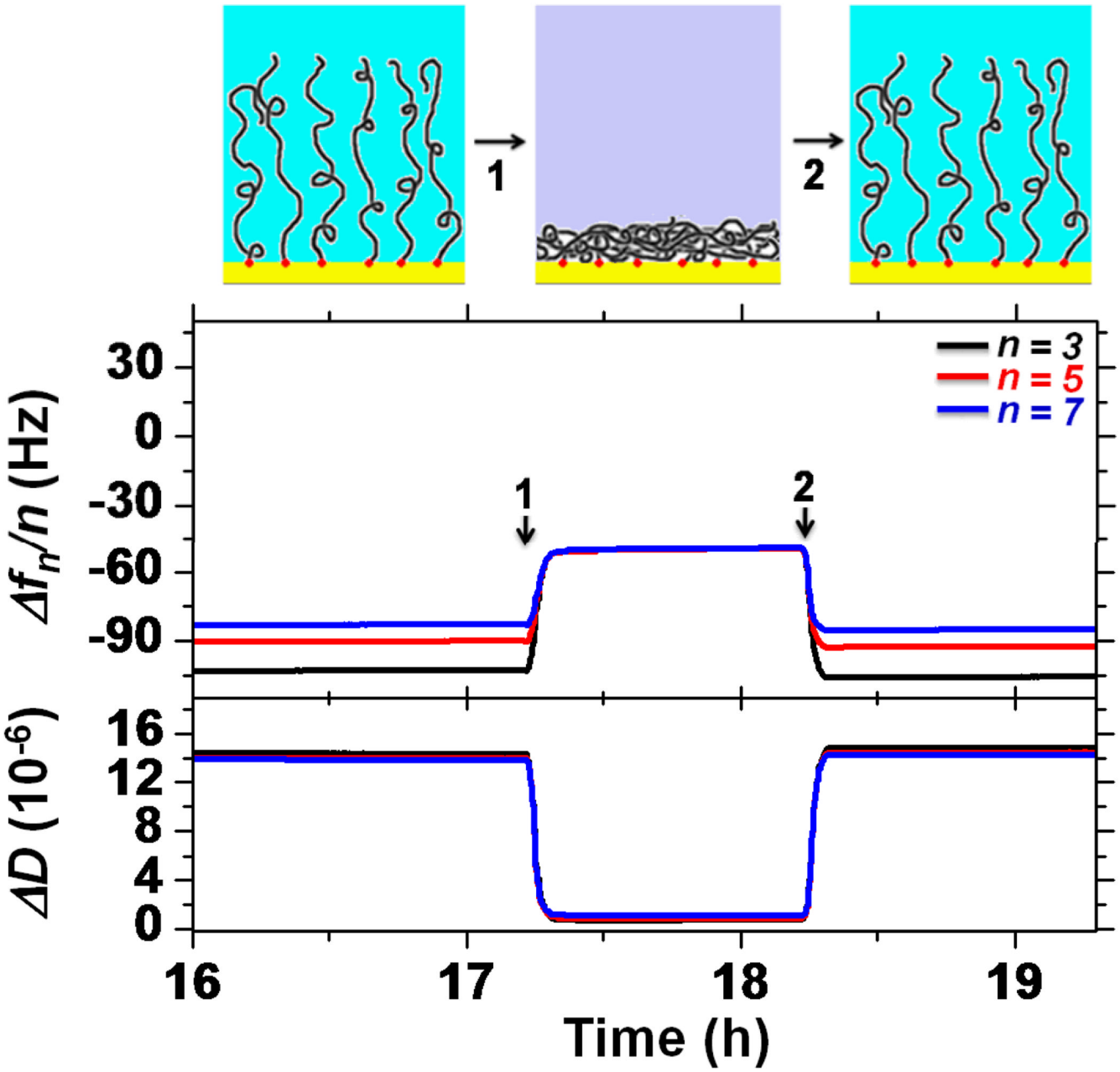

Fig. 1.

Response of frequency and dissipation in QCM-D technique to collapse of solvent-infused layer. The good solvent is changed to nonsolvent at arrow 1 and back at arrow 2 (reproduced with permission from Ref. 18)

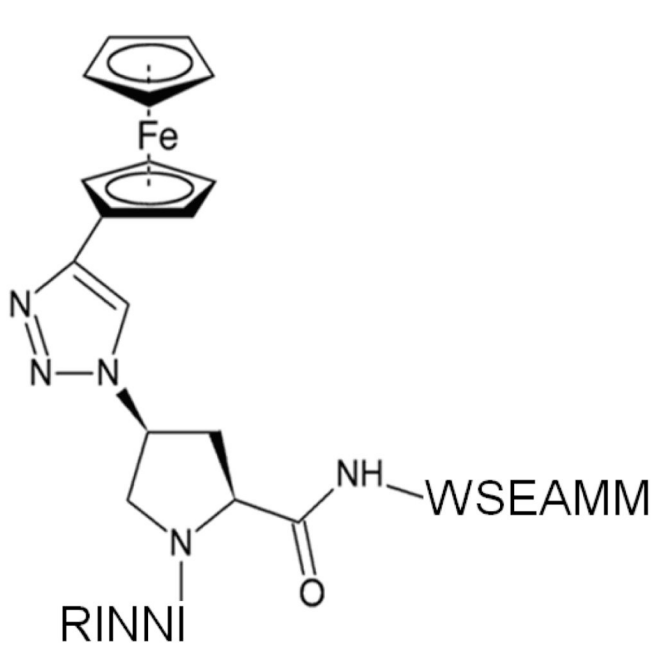

HNG-156

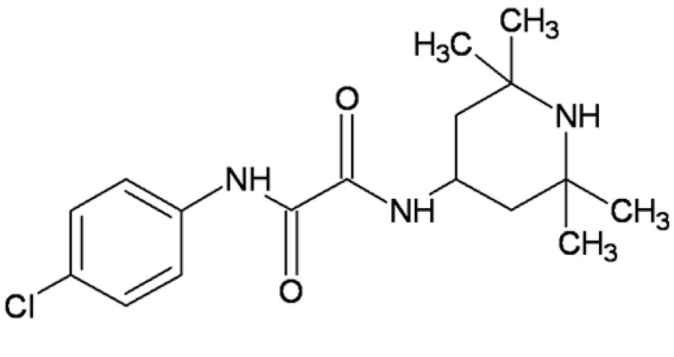

NBD-556

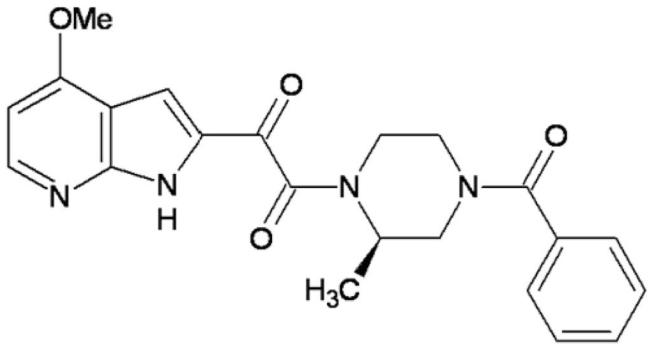

BMS-806

Fig. 2.

Chemical structures of small-molecule binding ligands. The sequences of letters, RINNI and WSEAMM represent amino acid sequences in which each amino acid is represented by its standard alphabetic symbol

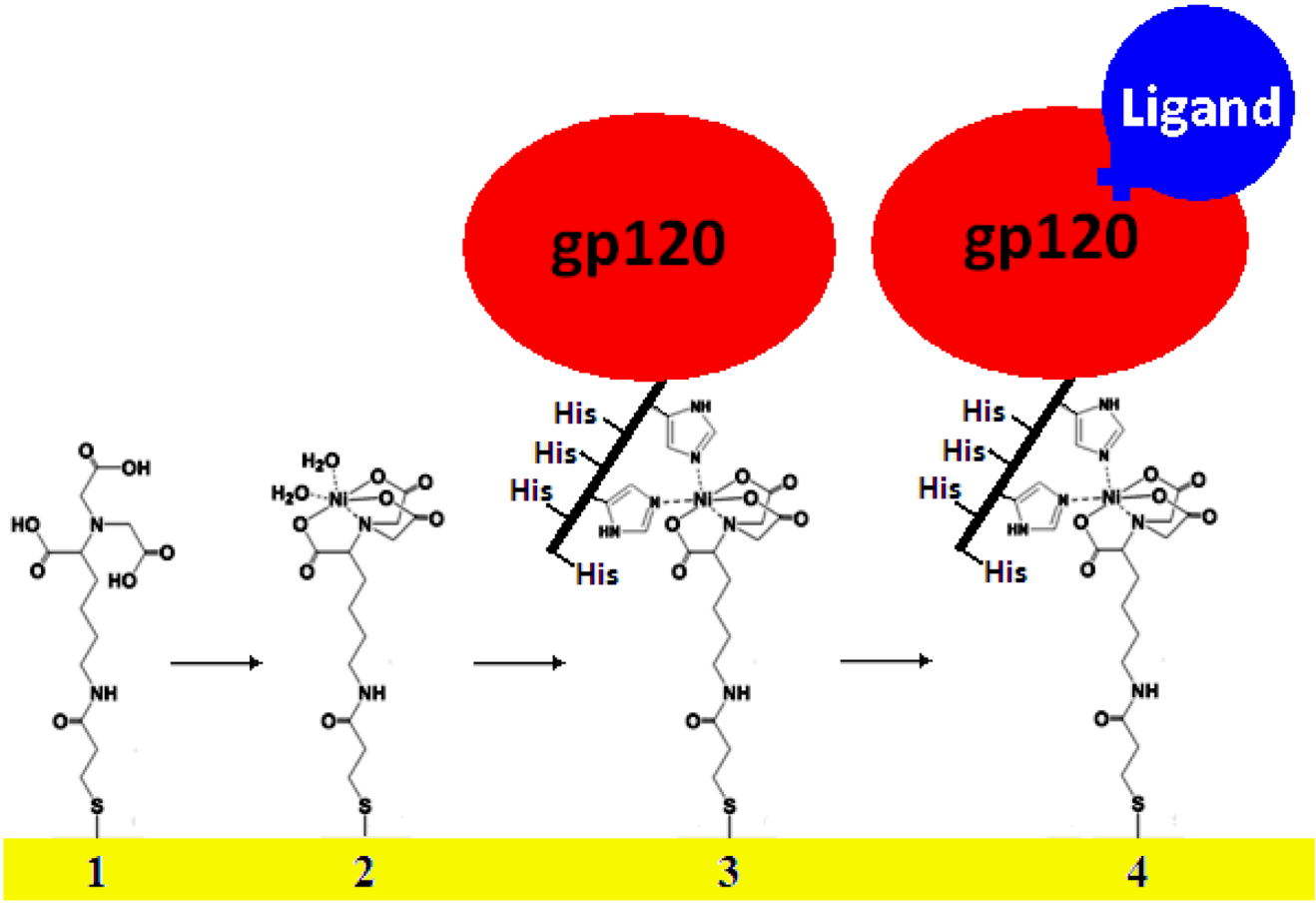

Fig. 3.

Overall scheme of steps taking place on the surface of the vibrating crystal in the QCM-D flow cell. (1) NTA is attached to gold-coated surface by means of thiol group, (2) coordination of Ni^{2+} with the neutralized acid groups of NTA, (3) immobilization of gp120 by coordination of histidine tag with Ni^{2+}, and (4) binding of ligand to gp120. The gp120 is disproportionately small in the figure

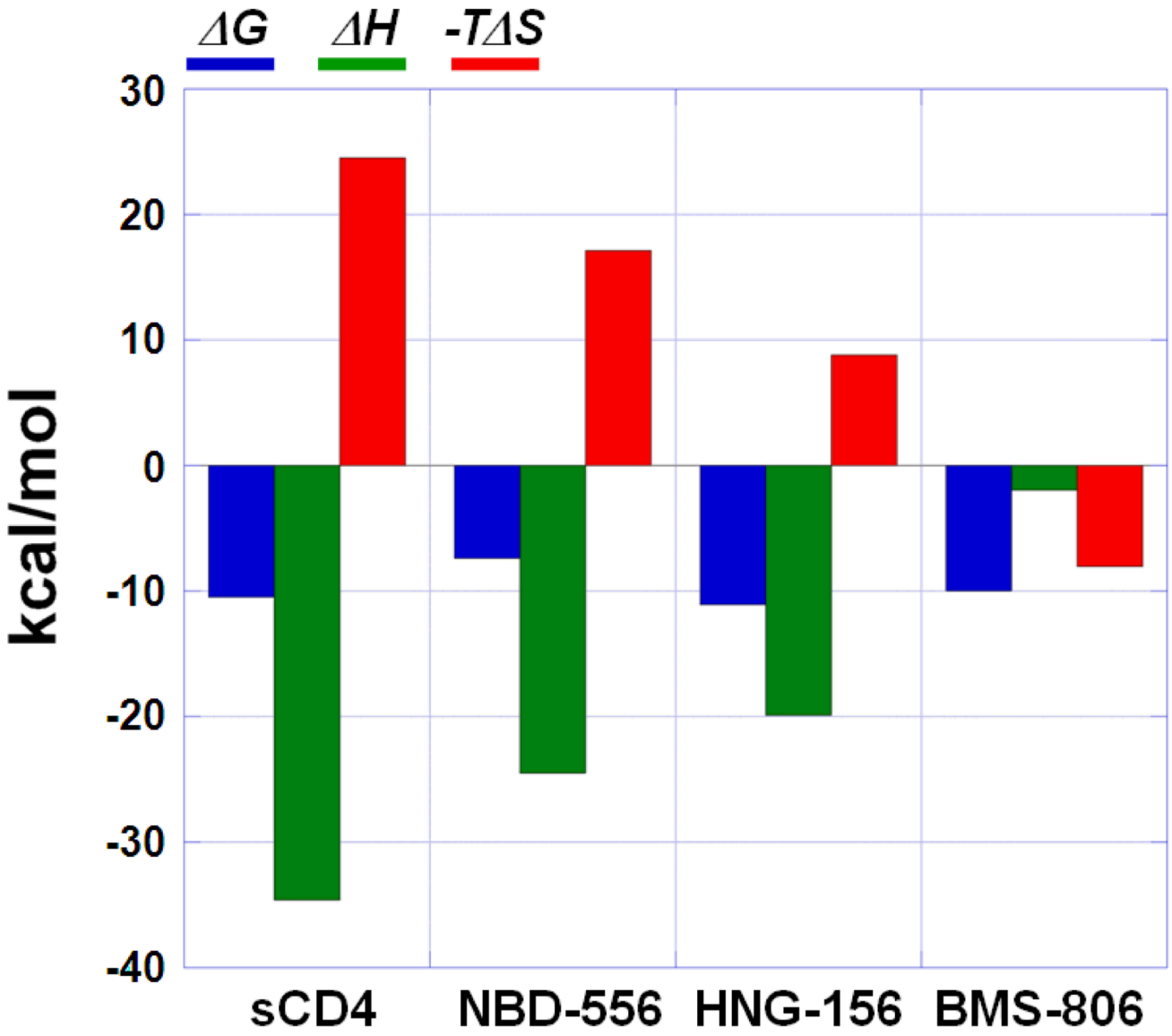

Fig. 4.

Graph of thermodynamic quantities for the binding of gp120 to various targets. Positive values of $-T\Delta S$ indicate a conformational ordering of the gp120. Data compiled from Ref. [32] for sCD4, Ref. [33] for NBD-556 and Ref. [34] for BMS-806. The data shown for HNG-156, obtained by the procedure of Ref. [34], have not been previously published.

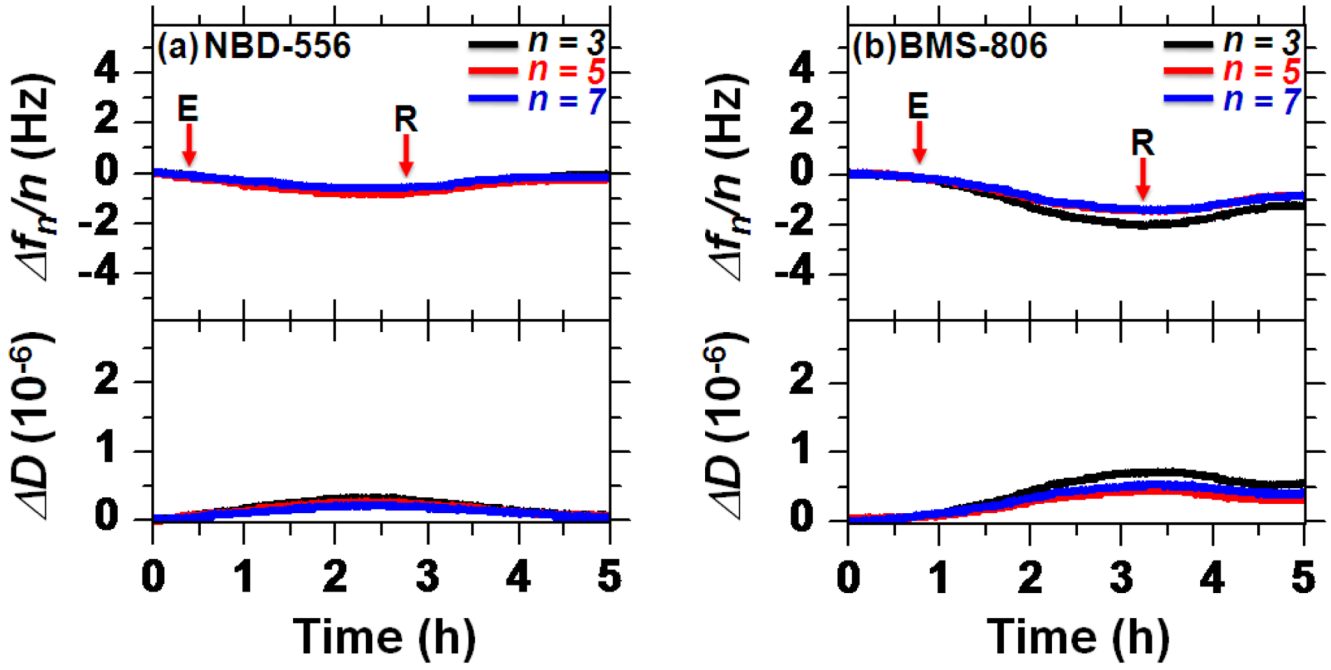

Fig. 5.

Traces of $\Delta f_n/n$ ($n = 3, 5, 7$) and ΔD vs. time for control experiments involving exposure of a solution of the ligand (a) NBD-556 and (b) BMS-806 to Ni-NTA-derivatized surface lacking immobilized gp120

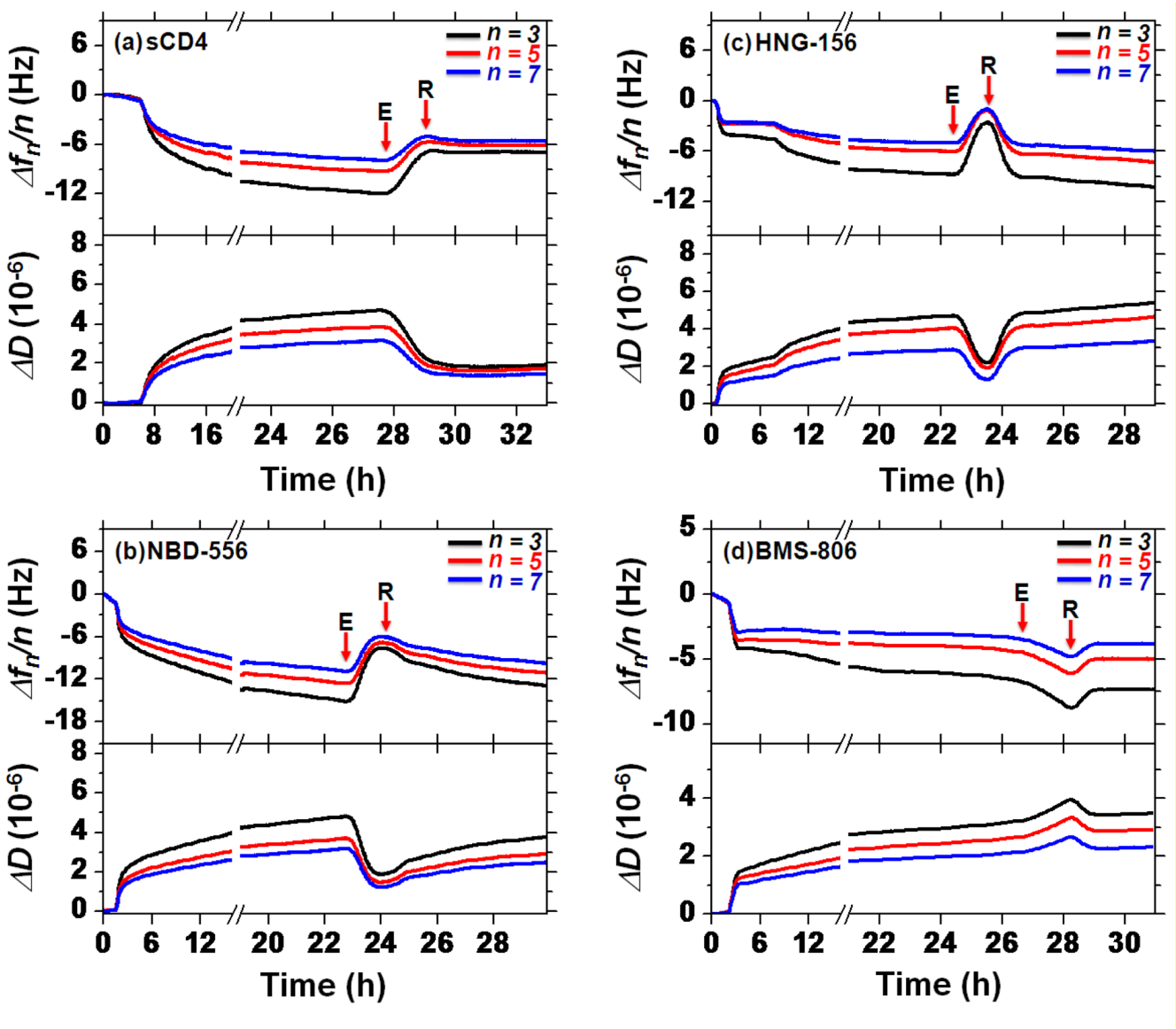

Fig. 6.

Traces of $\Delta f_n/n$ ($n = 3, 5, 7$) and ΔD vs. time for exposure of Ni-NTA-derivatized surface to a solution of gp120 in PBS, followed by exposure to sCD4, NBD-556, HNG-156, BMS-806 in PBS

Table 1

Characteristics of Ligand Solutions

Designation of ligand	M.W., g/mol	Solution conc., μ*M*
sCD4	45,200	1.0
HNG-156	1711	7.0
BMS-806	406.4	25
NBD-556	337.8	59